

Rectification of thermal fluctuations in ideal gases

P. Meurs,¹ C. Van den Broeck,¹ and A. Garcia²

¹*Limburgs Universitair Centrum, B-3590 Diepenbeek, Belgium*

²*Department of Physics, San Jose State University, San Jose, CA 95192-0106*

(Dated: 14th November 2018)

We calculate the systematic average speed of the adiabatic piston and a thermal Brownian motor, introduced in [Van den Broeck, Kawai and Meurs, *Microscopic analysis of a thermal Brownian motor*, to appear in Phys. Rev. Lett.], by an expansion of the Boltzmann equation and compare with the exact numerical solution.

PACS numbers: 05.20.Dd, 05.40.Jc, 05.60.Cd, 05.70.Ln

I. INTRODUCTION

Can thermal fluctuations be rectified? Ever since Maxwell [1] raised this question with his famous thought experiment involving a so-called Maxwell demon, it has been the object of debate in both the thermodynamics and statistical physics community. The mainstream opinion is that rectification is impossible in a system at equilibrium. Indeed the property of detailed balance, which was discovered by Onsager [2], and which turns out to be a basic characteristic of the steady state distribution in area preserving time-reversible dynamical systems (in particular Hamiltonian systems) [3], states that any transition between two states (defined as regions in phase space of nonzero measure and even in the speed) occurs as frequently as the time-reversed transition. The separate issue, first introduced by Szilard [4], of involving an “intelligent observer” that tracks the direction of these transitions, making possible the rectification by interventions at the right moment, has a contorted history of its own. It turns out that the engendered rectification is offset by the entropic cost of processing (and more precisely of erasing) the involved information [5]. Another more recent debate involving entangled quantum systems [6] is still ongoing.

Apart from the fundamental interest in the subject, a number of recent developments have put the issue of rectifying thermal fluctuations back on the agenda. First, we mention the observation that thermal fluctuations can in principle be rectified if the system under consideration operates under nonequilibrium conditions. The past decade has witnessed a surge in the literature on the subject of the so-called Brownian motors [7]. Such motors possibly explain, amongst other, phenomena such as transport and force generation in biological systems. Second, our ability to observe, manipulate or even fabricate objects on the nanoscale prompts us to look into new procedures to regulate such small systems, possibly by exploiting the effects of thermal fluctuations in a constructive way.

Even though several constructions have been envisaged to discuss the issue of rectification in more detail, including for example the Smoluchowski-Feynman ratchet [8], the issue of thermal fluctuations in a system with nonlinear friction [9] and the thermal diode [10, 11], no exactly solvable model has been put forward. In this paper, we will present two fully microscopic Hamiltonian models, in which the rectification of thermal fluctuations can be studied in analytic detail. Versions of the first model have appeared in the literature for some time under the name of Rayleigh piston [9] or adiabatic piston [12, 13, 14], see also [15]. The second model, to which we will refer as thermal Brownian motor, was introduced in a recent paper [16]. Both models involve a small object simultaneously in contact with two infinite reservoirs of ideal gases, each separately at equilibrium but possibly at a different temperature and/or density. A Boltzmann-Master equation provides a microscopically exact starting point to study the motion of the object. As a result of the rectification of the nonequilibrium fluctuations, the object acquires a systematic average speed, which will be calculated exactly via a perturbative solution of the Boltzmann equation, with the ratio of the mass of the gas particles over that of the object as the small parameter.

The organization of this paper is as follows. We start in section II by reviewing the general framework and the type of construction for the Brownian motor that we have in mind. The main technical ingredients are closely related to the so-called $1/\Omega$ -expansion of van Kampen [10]. In section III we turn to a detailed presentation and discussion of the adiabatic piston. The rectification has in this case been investigated to lowest order by Gruber and Piasecki [14]. We present a streamlined derivation allowing to go two orders further in the expansion. Next, in section IV, we discuss the more surprising thermal Brownian motor in which the motion derives from the spatial asymmetry of the object itself [16]. We again calculate the three first relevant terms in the expansion of the average speed. Finally, in section V, the obtained analytic results are compared with a direct numerical solution of the Boltzmann-Master equation and with previous molecular dynamics simulations [16].

II. EXPANSION OF THE BOLTZMANN-MASTER EQUATION

Consider a closed, convex and rigid object with a single degree of freedom, moving in a gas. To obtain a microscopically exact equation for the speed V of this object, we will consider the ideal gas limit in which:

- (1) the gas particles undergo instantaneous and perfectly elastic collisions with the object,
- (2) the mean free path of the particles is much larger than the linear dimensions of the object (regime of a large Knudsen number),
- (3) the (ideal) gas is initially at equilibrium, and hence at all times: the perturbation due to the collisions with the object are negligible in an infinitely large reservoir.

With these assumptions, there are no precollisional correlations between the speed of the object and those of the impinging gas particles, hence the Boltzmann ansatz of molecular chaos is exact [17]. In fact, since the collisions with the gas particles occur at random and uncorrelated in time, the speed V of the object is a Markov process and its probability density obeys a Boltzmann-Master equation of the following form:

$$\frac{\partial P(V, t)}{\partial t} = \int dV' \left[W(V|V')P(V', t) - W(V'|V)P(V, t) \right]. \quad (1)$$

$W(V|V')$ represents the transition probability per unit time to change the speed of the object from V' to V . Its detailed form can be easily obtained following arguments familiar from the kinetic theory of gases.

To construct a model for a Brownian motor, two additional ingredients need to be introduced. First we have to operate under nonequilibrium conditions. This can most easily be achieved by considering that the object interacts not with a single but with two ideal gases, both at equilibrium in a separate reservoir, each at its own temperature and density. The physical separation (no particle exchange) between the gases can be achieved by using the object itself as a barrier (adiabatic piston) or by assuming that the object consists out of two rigidly linked (closed and convex) units, each moving in one of the separate reservoirs containing the gases. Second, we need to break the spatial symmetry. In the adiabatic piston this is achieved by the asymmetric distribution of the gases with respect to the piston. In the thermal Brownian motor, at least one of the constitutive units needs to be spatially asymmetric. With these modifications in mind, we can still conclude that Eq. (1) remains valid, but the transition probability is now a sum of the contributions representing the collisions with the particles of each gas.

With the ingredients for a Brownian motor thus available, we expect that the object can rectify the fluctuating force resulting from the collisions with the gas particles. Hence it will develop a steady state average nonzero systematic speed, which we set out to calculate analytically. Unfortunately, an explicit exact solution of Eq. (1) cannot be obtained even at the steady state, and a perturbative solution is required. Since we expect that the rectification disappears in the limit of a macroscopic object, a natural expansion parameter is the ratio of the mass m of the gas particle over the mass M of the object. More precisely, we will use $\varepsilon = \sqrt{m/M}$ as the expansion parameter. In fact this type of expansion is very familiar for the equilibrium version of the adiabatic piston, namely the so-called Rayleigh particle. It has been developed with the primary aim of deriving exact Langevin equations from microscopic theory and culminated in the more general well-known $1/\Omega$ expansion of van Kampen [10]. With the aim of streamlining this procedure for the direct calculation of the average drift velocity, with special attention to higher order corrections, we briefly review the technical details. First it is advantageous to introduce the transition probability $W(V'; r) = W(V|V')$, defined in terms of the jump amplitude $r = V - V'$, since the latter jumps are anticipated to become small in the limit $\varepsilon \rightarrow 0$. One can then rewrite the Master equation as follows:

$$\frac{\partial P(V, t)}{\partial t} = \int W(V - r; r)P(V - r, t)dr - P(V, t) \int W(V; -r)dr. \quad (2)$$

A Taylor expansion of the transition probability in the first integral of Eq. (2) with respect to the jump amplitude leads to an equivalent expression under the form of the Kramers-Moyal expansion:

$$\frac{\partial P(V, t)}{\partial t} = \sum_{n=1}^{\infty} \frac{(-1)^n}{n!} \left(\frac{d}{dV} \right)^n \{a_n(V)P(V, t)\}, \quad (3)$$

with the so-called ‘‘jump moments’’ given by

$$a_n(V) = \int r^n W(V; r)dr. \quad (4)$$

Since the change in the speed of our object of mass M , i.e., the jump amplitude r , will, upon colliding with a particle of mass m , be of order $\varepsilon^2 = m/M$, the Kramers-Moyal expansion appears to provide the requested expansion

in our small parameter. However, the parameter M will also appear implicitly in the speed V . Indeed, we expect that the object will, in the stationary regime, exhibit thermal fluctuations at an effective temperature T_{eff} , i.e., $\frac{1}{2}M\langle V^2 \rangle = \frac{1}{2}k_B T_{\text{eff}}$. To take this into account, we switch to a dimensionless variable x of order 1:

$$x = \sqrt{\frac{M}{k_B T_{\text{eff}}}} V. \quad (5)$$

The explicit value of T_{eff} will be determined below by self-consistency, more precisely from the condition $\langle x^2 \rangle = 1$ to first order in ε . The probability density $P(x, t)$ for the new variable x thus obeys the following equation:

$$\frac{\partial P(x, t)}{\partial t} = \sum_{n=1}^{\infty} \frac{(-1)^n}{n!} \left(\frac{d}{dx} \right)^n \{A_n(x)P(x, t)\}, \quad (6)$$

with rescaled jump moments, $A_n(x)$, defined as

$$A_n(x) = \left(\sqrt{\frac{M}{k_B T_{\text{eff}}}} \right)^n a_n(x). \quad (7)$$

Equivalently, and of more interest to us, the following set of coupled equations determine the moments $\langle x^n \rangle = \int x^n P(x, t) dx$:

$$\begin{aligned} \partial_t \langle x \rangle &= \langle A_1(x) \rangle \\ \partial_t \langle x^2 \rangle &= 2\langle x A_1(x) \rangle + \langle A_2(x) \rangle \\ \partial_t \langle x^3 \rangle &= 3\langle x^2 A_1(x) \rangle + 3\langle x A_2(x) \rangle + \langle A_3(x) \rangle \\ \partial_t \langle x^4 \rangle &= 4\langle x^3 A_1(x) \rangle + 6\langle x^2 A_2(x) \rangle + 4\langle x A_3(x) \rangle + \langle A_4(x) \rangle \\ \partial_t \langle x^5 \rangle &= 5\langle x^4 A_1(x) \rangle + 10\langle x^3 A_2(x) \rangle + 10\langle x^2 A_3(x) \rangle + 5\langle x A_4(x) \rangle + \langle A_5(x) \rangle \\ \partial_t \langle x^6 \rangle &= 6\langle x^5 A_1(x) \rangle + 15\langle x^4 A_2(x) \rangle + 20\langle x^3 A_3(x) \rangle + 15\langle x^2 A_4(x) \rangle + 6\langle x A_5(x) \rangle + \langle A_6(x) \rangle \\ &\dots \end{aligned} \quad (8)$$

The exact solution of this coupled set of equations is as hopeless and equally difficult as the full Boltzmann-Master equation. However, a Taylor expansion in ε shows that the equations are no longer fully coupled and the calculation of a moment up to a finite order reduces to an in principle simple (but in practice tedious) algebraic problem.

III. THE ADIABATIC PISTON

A. Motivation

In Fig. 1, we have represented in a schematic way the construction of the Rayleigh piston and of its nonequilibrium version known as the adiabatic piston. We concentrate here on an (infinite) two-dimensional system, for reasons of simplicity. The piston is considered to be a single “flat” particle of length L and mass M with a unique degree of freedom, namely its position x along the horizontal axis. Since the piston has no internal degrees of freedom, it can not transfer energy by “hidden” microscopic degrees of freedom. The absence of a corresponding heat exchange prompted the use of the name “adiabatic piston”. The piston is moving inside an infinite rectangle separating the gases to its right and left from each other. These gases are initially taken separately in equilibrium, but not necessarily at equilibrium with each other. In the thermodynamic context of a macroscopic piston, this construction is an example of an indeterminate problem, i.e., the final position of the piston can not be predicted by the criterion of maximizing the total entropy, since it depends on the initial preparation of the gases [13], see also [14]. The case of interest to us is when the mass of the piston is not macroscopically large, i.e., finite $\varepsilon = \sqrt{m/M}$. When operating furthermore at equilibrium, this Rayleigh piston provides an exactly solvable model, allowing for example, the rigorous derivation of a linear Langevin equation appearing as the first nontrivial limit of the Boltzmann-Master equation in the limit $\varepsilon \rightarrow 0$. When the left and right gases are not at equilibrium, but exert equal pressure on the piston, the model becomes an example of a Brownian motor, which is able to perform work by rectifying pressure fluctuations [14]. In doing so, the single degree of freedom x also plays the role of a microscopic thermal conductivity, an issue that is quite relevant to other models of Brownian motors [18]. Since this model is essentially one-dimensional and the related calculations are relatively simple, we include it in this paper to illustrate the calculation procedure and at the same time to derive novel results for the average drift speed up to order ε^5 .

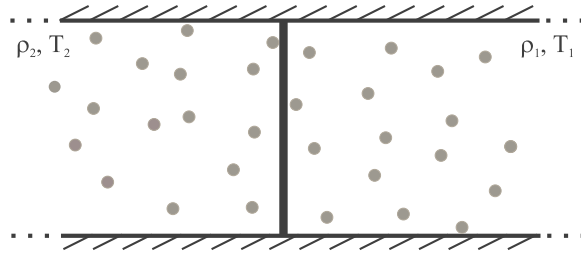


Figure 1: The adiabatic piston.

B. Presentation of the model

The ideal gases in the right and left compartments, separated from each other by the piston, are each at equilibrium with Maxwellian velocity distributions at temperatures T_1 and T_2 , and with uniform particle densities ρ_1 and ρ_2 , respectively. Since we are mainly interested in the rectification of fluctuations, we will focus on the case of mechanical equilibrium with equal pressure on both sides of the piston, i.e., $\rho_1 T_1 = \rho_2 T_2$.

The motion of the piston is determined by the laws of Newton. Hence its velocity only changes, say from V' to V , when it undergoes a collision with a gas particle, its (x -component of the) velocity going from v'_x to v_x . Conservation of energy and momentum determines the post-collisional speeds in terms of the pre-collisional ones:

$$\begin{aligned} \frac{1}{2}mv_x^2 + \frac{1}{2}MV^2 &= \frac{1}{2}mv_x'^2 + \frac{1}{2}MV'^2 \\ mv_x + MV &= mv_x' + MV', \end{aligned}$$

implying:

$$V = V' + \frac{2m}{m+M}(v'_x - V'). \quad (9)$$

The transition probability $W(V|V')$ then follows from standard arguments in kinetic theory of gases: one evaluates the frequency of collisions of gas particles of a given speed and subsequently integrates over all the speeds. Note that we have two separate contributions from the gas right (ρ_1 and T_1) and left (ρ_2 and T_2). The result reads:

$$W(V|V') = \begin{cases} L\rho_1 \int_{-\infty}^{+\infty} dv_x (v_x - V') H[v_x - V'] \phi_1(v_x) \delta \left[V' + \frac{2m}{m+M}(v_x - V') - V \right] & \text{if } V < V' \\ L\rho_2 \int_{-\infty}^{+\infty} dv_x (V' - v_x) H[V' - v_x] \phi_2(v_x) \delta \left[V' + \frac{2m}{m+M}(v_x - V') - V \right] & \text{if } V > V', \end{cases}$$

with H the Heaviside function, δ the Dirac distribution and ϕ_i the Maxwell-Boltzmann distribution at temperature T_i :

$$\phi_i(v_x) = \sqrt{\frac{m}{2\pi k_B T_i}} \exp\left(\frac{-mv_x^2}{2k_B T_i}\right).$$

Performing the integrals over the speed gives the following explicit result for the transition probability:

$$\begin{aligned} W(V|V') &= L\rho_1 \left[\frac{m+M}{2m} \right]^2 (V' - V) H[V' - V] \phi_1\left(V' - \frac{m+M}{2m}(V' - V)\right) \\ &+ L\rho_2 \left[\frac{m+M}{2m} \right]^2 (V - V') H[V - V'] \phi_2\left(V' - \frac{m+M}{2m}(V' - V)\right). \end{aligned} \quad (10)$$

From the transition probability, the rescaled jump moments $A_n(x)$ (7) can be calculated. The exact expression for the n -th jump moment is as follows :

$$\begin{aligned}
A_n(x) = & 2^{(3n-1)/2} L \sqrt{\frac{k_B}{\pi m}} \frac{\varepsilon^n}{(1+\varepsilon^2)^n} T_{\text{eff}}^{-n/2} \Gamma\left[\frac{2+n}{2}\right] \left((-1)^n \rho_1 T_1^{(n+1)/2} \exp\left[-\frac{T_{\text{eff}}}{2T_1} x^2 \varepsilon^2\right] \Phi\left[\frac{2+n}{2}, \frac{1}{2}, \frac{T_{\text{eff}}}{2T_1} x^2 \varepsilon^2\right] \right. \\
& \left. + \rho_2 T_2^{(n+1)/2} \exp\left[-\frac{T_{\text{eff}}}{2T_2} x^2 \varepsilon^2\right] \Phi\left[\frac{2+n}{2}, \frac{1}{2}, \frac{T_{\text{eff}}}{2T_2} x^2 \varepsilon^2\right] \right) \\
& + 2^{3n/2} L \sqrt{\frac{k_B}{\pi m}} \frac{\varepsilon^{n+1}}{(1+\varepsilon^2)^n} T_{\text{eff}}^{(1-n)/2} \Gamma\left[\frac{3+n}{2}\right] x \left((-1)^n \rho_1 T_1^{n/2} \exp\left[-\frac{T_{\text{eff}}}{2T_1} x^2 \varepsilon^2\right] \Phi\left[\frac{3+n}{2}, \frac{3}{2}, \frac{T_{\text{eff}}}{2T_1} x^2 \varepsilon^2\right] \right. \\
& \left. - \rho_2 T_2^{n/2} \exp\left[-\frac{T_{\text{eff}}}{2T_2} x^2 \varepsilon^2\right] \Phi\left[\frac{3+n}{2}, \frac{3}{2}, \frac{T_{\text{eff}}}{2T_2} x^2 \varepsilon^2\right] \right), \tag{11}
\end{aligned}$$

with Γ the Gamma function:

$$\begin{aligned}
\Gamma[1+k] &= k! \\
\Gamma\left[1 + \frac{2k+1}{2}\right] &= \frac{\sqrt{\pi}}{2^{k+1}} 1 \cdot 3 \cdot 5 \cdot \dots \cdot (2k+1), \tag{12}
\end{aligned}$$

and Φ the Kummer function, in its integral representation given by

$$\Phi[a, b, z] = \frac{\Gamma[b]}{\Gamma[b-a]\Gamma[a]} \int_0^1 e^{zt} t^{a-1} (1-t)^{b-a-1} dt. \tag{13}$$

C. Stationary speed

The moment equations (8) form together with the explicit expressions (11) for the jump moments the starting point for a straightforward perturbation in terms of the small parameter ε . To simplify notation, we introduce:

$$f(n) = L \sqrt{\frac{2}{\pi}} \sqrt{\frac{k_B}{m}} \frac{\rho_1 T_1^n + \rho_2 T_2^n}{T_{\text{eff}}^{n-\frac{1}{2}}} \tag{14}$$

$$g(n) = L \sqrt{\frac{k_B}{m}} \frac{\rho_1 T_1^n - \rho_2 T_2^n}{T_{\text{eff}}^{n-\frac{1}{2}}}. \tag{15}$$

Also, the limit $\varepsilon \rightarrow 0$ entails a slowing down of the motion of the piston, which can be accounted for by introducing a new scaled time variable:

$$\tau = \varepsilon^2 t.$$

The equations for the first and second moment, expanded up to order ε^5 and ε^4 respectively, are as follows (the expansion for higher moments up to the sixth moment can be found in appendix A):

$$\begin{aligned}
\partial_\tau \langle x \rangle = & -2 f[1/2] \langle x \rangle - g[0] \langle x^2 \rangle \varepsilon + \frac{1}{3} (6 f[1/2] \langle x \rangle - f[-1/2] \langle x^3 \rangle) \varepsilon^2 \\
& + g[0] \langle x^2 \rangle \varepsilon^3 + \left(-2 f[1/2] \langle x \rangle + \frac{1}{3} f[-1/2] \langle x^3 \rangle + \frac{1}{60} f[-3/2] \langle x^5 \rangle \right) \varepsilon^4 - g[0] \langle x^2 \rangle \varepsilon^5 + O(\varepsilon^6) \tag{16}
\end{aligned}$$

$$\begin{aligned}
\partial_\tau \langle x^2 \rangle = & 4 (f[3/2] - f[1/2] \langle x^2 \rangle) - 2 g[0] \langle x^3 \rangle \varepsilon + 2 \left(-4 f[3/2] + 5 f[1/2] \langle x^2 \rangle - \frac{1}{3} f[-1/2] \langle x^4 \rangle \right) \varepsilon^2 \\
& + 4 g[0] \langle x^3 \rangle \varepsilon^3 + \left(12 f[3/2] - 16 f[1/2] \langle x^2 \rangle + \frac{7}{6} f[-1/2] \langle x^4 \rangle + \frac{1}{30} f[-3/2] \langle x^6 \rangle \right) \varepsilon^4 + O(\varepsilon^5). \tag{17}
\end{aligned}$$

Note that the condition of macroscopic equilibrium ($\rho_1 T_1 = \rho_2 T_2$) was used to derive these equations. In particular, without this constraint, an additional term corresponding to a constant, velocity-independent, force acting on the piston, would be present in Eq. (16).

To lowest order in ε , the equation for the first moment, Eq. (16), is not coupled to higher order moments. It

displays the usual linear relaxation term of the velocity, namely, in original variables, $M\partial_t\langle V \rangle = -\gamma\langle V \rangle$, with friction coefficient γ :

$$\gamma = 4L\sqrt{\frac{k_B m}{2\pi}} \left(\rho_1\sqrt{T_1} + \rho_2\sqrt{T_2} \right). \quad (18)$$

For $T_1 = T_2$ and (consequently) $\rho_1 = \rho_2$, this result is in agreement with [10]. We conclude that at this order of the perturbation, the steady state speed is zero. This is not surprising since any asymmetry is buried at the level of linear response theory.

Going beyond the lowest order, one enters into the domain where fluctuations and nonlinearity are intertwined. The first moment is now coupled to the higher order moments. Therefore, we focus on the steady state speed reached by the piston in the long time limit. We will omit, for simplicity of notation, a superscript *st* to refer to this stationary regime. Recalling that we defined the effective temperature T_{eff} by the condition $\langle x^2 \rangle = 1$ at the lowest order in ε , we immediately find from Eq. (16) that at order ε the piston will indeed develop a nonzero average systematic speed equal to $\varepsilon g(0)/[2f(1/2)]$. The explicit value of T_{eff} follows from Eq. (17), implying at lowest order in ε that $\langle x^2 \rangle = f(3/2)/f(1/2) = 1$. In original variables, cf. Eq. (5), these results read as follows:

$$T_{\text{eff}} = \sqrt{T_1 T_2} \quad (19)$$

and

$$\langle V \rangle = \frac{\sqrt{2\pi}}{4} \sqrt{\frac{m}{M}} \left(\sqrt{\frac{k_B T_1}{M}} - \sqrt{\frac{k_B T_2}{M}} \right) + \dots \quad (20)$$

Although there is no macroscopic force present (pressures on both sides of the piston are equal), the piston attains a stationary state with a non-zero average velocity toward the higher temperature region. Fluctuations conspire with the spatial asymmetry to induce a net motion in the absence of macroscopic forces. It is also clear from Eq.(20) that the net motion vanishes when $T_1 = T_2$ and also in the macroscopic limit $M \rightarrow \infty$. The above result was already derived in [14], but the calculation presented here is streamlined so as to allow for a swift calculation of higher order corrections.

At each of the next orders, a coupling arises to a next higher order moment. We shall present here the results up to order ε^5 , requiring the evaluation of the moments $\langle x^2 \rangle$, $\langle x^3 \rangle$, $\langle x^4 \rangle$, $\langle x^5 \rangle$ and $\langle x^6 \rangle$, up to orders ε^4 , ε^3 , ε^2 , ε^1 and ε^0 , respectively (cf. appendix A for details of the calculation). The resulting expression for the average stationary speed in the original variable V up to fifth order in ε is:

$$\begin{aligned} \langle V \rangle = & \left(\frac{m}{M} \right)^{1/2} \sqrt{\frac{\pi k_B}{2M}} \frac{1}{2} \left(\sqrt{T_1} - \sqrt{T_2} \right) \\ & + \left(\frac{m}{M} \right)^{3/2} \sqrt{\frac{\pi k_B}{2M}} \left(\frac{1}{4} \left(\sqrt{T_1} - \sqrt{T_2} \right) - \frac{1}{3} \frac{\rho_1 \sqrt{T_2} + \rho_2 \sqrt{T_1}}{\rho_1 \sqrt{T_1} + \rho_2 \sqrt{T_2}} \left(\sqrt{T_1} - \sqrt{T_2} \right) + \frac{\pi}{16} \frac{\left(\sqrt{T_1} - \sqrt{T_2} \right)^3}{\sqrt{T_1 T_2}} \right) \\ & + \left(\frac{m}{M} \right)^{5/2} \sqrt{\frac{\pi k_B}{2M}} \frac{1}{8} \left(\left(\sqrt{T_1} - \sqrt{T_2} \right) - 5 \frac{\left(\rho_1 T_1^{-1/2} + \rho_2 T_2^{-1/2} \right)^2 T_1 T_2 \left(\sqrt{T_1} - \sqrt{T_2} \right)}{\left(\rho_1 \sqrt{T_1} + \rho_2 \sqrt{T_2} \right)^2} \right. \\ & \left. + \frac{85}{18} \frac{\rho_1 \sqrt{T_2} + \rho_2 \sqrt{T_1}}{\rho_1 \sqrt{T_1} + \rho_2 \sqrt{T_2}} \left(\sqrt{T_1} - \sqrt{T_2} \right) + \frac{1}{3} \frac{\rho_1 T_1^{-3/2} + \rho_2 T_2^{-3/2}}{\rho_1 \sqrt{T_1} + \rho_2 \sqrt{T_2}} T_1 T_2 \left(\sqrt{T_1} - \sqrt{T_2} \right) - \frac{29\pi}{12} \frac{\left(\sqrt{T_1} - \sqrt{T_2} \right)^3}{\sqrt{T_1 T_2}} \right. \\ & \left. + \frac{47\pi}{12} \frac{\left(\rho_1 T_1^{-1/2} + \rho_2 T_2^{-1/2} \right) \left(\sqrt{T_1} - \sqrt{T_2} \right)^3}{\left(\rho_1 \sqrt{T_1} + \rho_2 \sqrt{T_2} \right)} - \frac{3\pi^2}{4} \frac{\left(\sqrt{T_1} - \sqrt{T_2} \right)^5}{T_1 T_2} \right) + \dots \quad (21) \end{aligned}$$

As required, the average speed is zero at equilibrium, when $T_1 = T_2$. Note also that the average speed depends on the densities of the gases solely through their ratio ρ_1/ρ_2 . This implies that, for T_1 and T_2 fixed, varying the densities will not modify the steady-state velocity when operating at mechanical equilibrium. In Fig. 2a. and Fig. 2b., we illustrate the dependence of $\langle V \rangle$ on the temperatures: the piston always moves towards the high temperature region and its speed increases with the temperature difference.

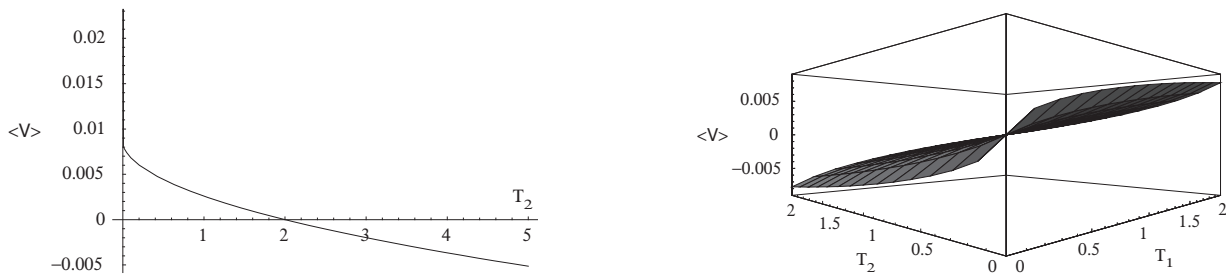


Figure 2: Stationary average speed of the adiabatic piston according to Eq. (21). Left: For $\rho_1 = 0.25$ and $T_1 = 2.0$ fixed, the speed is shown as a function of T_2 . Note that ρ_2 is determined by the condition of mechanical equilibrium ($\rho_1 T_1 = \rho_2 T_2$) and that the piston always moves to the higher temperature region. Right: the speed of the piston as a function of T_1 and T_2 , for $\rho_1 = 0.25$ and $\rho_2 = \rho_1 T_1 / T_2$. The velocity vanishes when $T_1 = T_2$ and is maximal for a large temperature difference. The following parameter values were used: mass of the gas particles $m = 1$, mass of the piston $M = 100$ and $k_B = 1$ by choice of units.

IV. THERMAL BROWNIAN MOTOR

A. Motivation

The systematic motion observed in the adiabatic piston is not entirely surprising since the piston is embedded in a nonequilibrium state with an explicit spatial asymmetry of its surroundings. More interesting is the case of the thermal Brownian motor, which was introduced and studied by molecular dynamics in a recent paper [16]. While the spatial environment is perfectly symmetric here, the object itself has a spatial asymmetry. The nonequilibrium conditions are generated by its interaction with two (or more) ideal gases that are not at the same temperature. The perturbative analysis, presented for the adiabatic piston, can be repeated here but is more involved because the problem is now genuinely two-dimensional.

B. Presentation of the model

Consider a 2-dimensional convex and closed object with total circumference S . Suppose that dS is a small part of the surface, inclined at an angle θ , measured counterclockwise from the x -axis (see Fig. 3). We define the form factor $F(\theta)$ as the fraction of the surface with orientation θ . This means that $SF(\theta)d\theta$ is the length of the surface with orientation between θ and $\theta + d\theta$. One can immediately verify that F satisfies

$$\begin{cases} F(\theta) \geq 0 & \text{positivity} & \text{(a)} \\ \int_0^{2\pi} d\theta F(\theta) = 1 & \text{normalization} & \text{(b)} \\ \int_0^{2\pi} d\theta F(\theta) \sin \theta = \int_0^{2\pi} d\theta F(\theta) \cos \theta = 0 & \text{object is closed.} & \text{(c)} \end{cases} \quad (22)$$

To simplify notation we will write $\langle \sin \theta \rangle$ instead of $\int_0^{2\pi} d\theta F(\theta) \sin \theta$.

We suppose that the object, with total mass M and velocity \vec{V} , has no rotational degree of freedom and a single translational degree of freedom. Choosing the latter oriented following the x -axis, we can write $\vec{V} = (V, 0)$. Collisions of the gas particles, of mass m and velocity \vec{v} , with the object are supposed to be instantaneous and perfectly elastic. Hence, pre-collisional and post-collisional velocities of the object, V' and V , and of a gas particle, $\vec{v}' = (v'_x, v'_y)$ and $\vec{v} = (v_x, v_y)$, are linked by conservation of the total energy and the momentum in the x -direction,

$$\frac{1}{2}MV'^2 + \frac{1}{2}mv_x'^2 + \frac{1}{2}mv_y'^2 = \frac{1}{2}MV^2 + \frac{1}{2}mv_x^2 + \frac{1}{2}mv_y^2 \quad (23)$$

$$mv_x' + MV' = mv_x + MV. \quad (24)$$

Furthermore, we assume a (short-range) central force, implying that the component of the momentum of the gas particle along the contact surface of the object is conserved:

$$\vec{v}' \cdot \vec{e}_{\parallel} = \vec{v} \cdot \vec{e}_{\parallel}, \quad (25)$$

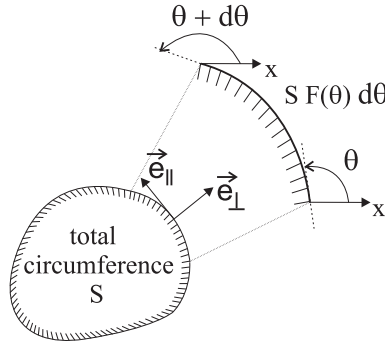


Figure 3: A closed and convex object with total circumference S . The length of the surface with an orientation between θ and $\theta + d\theta$ is $SF(\theta)d\theta$, defining the form factor $F(\theta)$.

with $\vec{e}_{\parallel} = (\cos\theta, \sin\theta)$, see Fig. 3. This yields for the post-collisional speed V :

$$V = V' + \frac{2\frac{m}{M}\sin^2\theta}{1 + \frac{m}{M}\sin^2\theta} (v'_x - V' - v'_y \cot\theta). \quad (26)$$

Similar as in the adiabatic piston problem, we start from the linear Boltzmann equation (1), which is exact in the ideal gas limit, to describe the motion of the object. The object consists out of rigidly linked (closed and convex) parts, each sitting in a reservoir i containing an ideal gas with uniform particle density ρ_i and Maxwellian velocity distribution ϕ_i at temperature T_i :

$$\phi_i(v_x, v_y) = \frac{m}{2\pi k_B T_i} \exp\left(\frac{-m(v_x^2 + v_y^2)}{2k_B T_i}\right). \quad (27)$$

Examples of the construction with two reservoirs are schematically represented in Fig. 4. The transition probability $W(V|V')$ is then the sum of the contributions of the different units of the object and can be calculated, starting from the basic arguments of the kinetic theory. The contribution dW_i to $W(V|V')$ of the surface section of size dS_i , with orientation in $[\theta, \theta + d\theta]$, exposed to the gas mixture i is

$$\begin{aligned} dW_i(V|V') &= S_i F_i(\theta) d\theta \int_{-\infty}^{+\infty} dv'_x \int_{-\infty}^{+\infty} dv'_y H[(\vec{V}' - \vec{v}') \cdot \vec{e}_{\perp}] |(\vec{V}' - \vec{v}') \cdot \vec{e}_{\perp}| \\ &\rho_i \phi_i(v'_x, v'_y) \delta\left[V - V' - \frac{2\frac{m}{M}\sin^2\theta}{1 + \frac{m}{M}\sin^2\theta} (v'_x - V' - v'_y \cot\theta)\right], \end{aligned} \quad (28)$$

with H the Heaviside function, δ the Dirac distribution and $\vec{e}_{\perp} = (\sin\theta, -\cos\theta)$ a unit vector normal to the surface, see Fig. 3. The total transition probability is then given by

$$W(V|V') = \sum_i \int_0^{2\pi} dW_i(V|V'). \quad (29)$$

The integrals over the speed of the colliding gas particles can be performed explicitly, resulting in:

$$\begin{aligned} W(V|V') &= \frac{1}{4} \sum_i S_i \rho_i \sqrt{\frac{m}{2\pi k_B T_i}} \left((V' - V) H[V' - V] \int_{\sin\theta > 0} + (V - V') H[V - V'] \int_{\sin\theta < 0} \right) \\ &d\theta F_i(\theta) \left(\frac{M}{m \sin\theta} + \sin\theta \right)^2 \exp\left[-\frac{m(V' + \frac{1}{2}[(V - V')(1 + \frac{M}{m \sin^2\theta})])^2 \sin^2\theta}{2k_B T_i}\right]. \end{aligned} \quad (30)$$

The remaining integral depends on the shape of the object.

Following the general set-up, we switch to the dimensionless variable $x = \sqrt{\frac{M}{k_B T_{\text{eff}}}} V$, cf. (5), with the effective temperature T_{eff} to be determined from the condition $\langle x^2 \rangle = 1$. The exact expression for the n -th rescaled jump

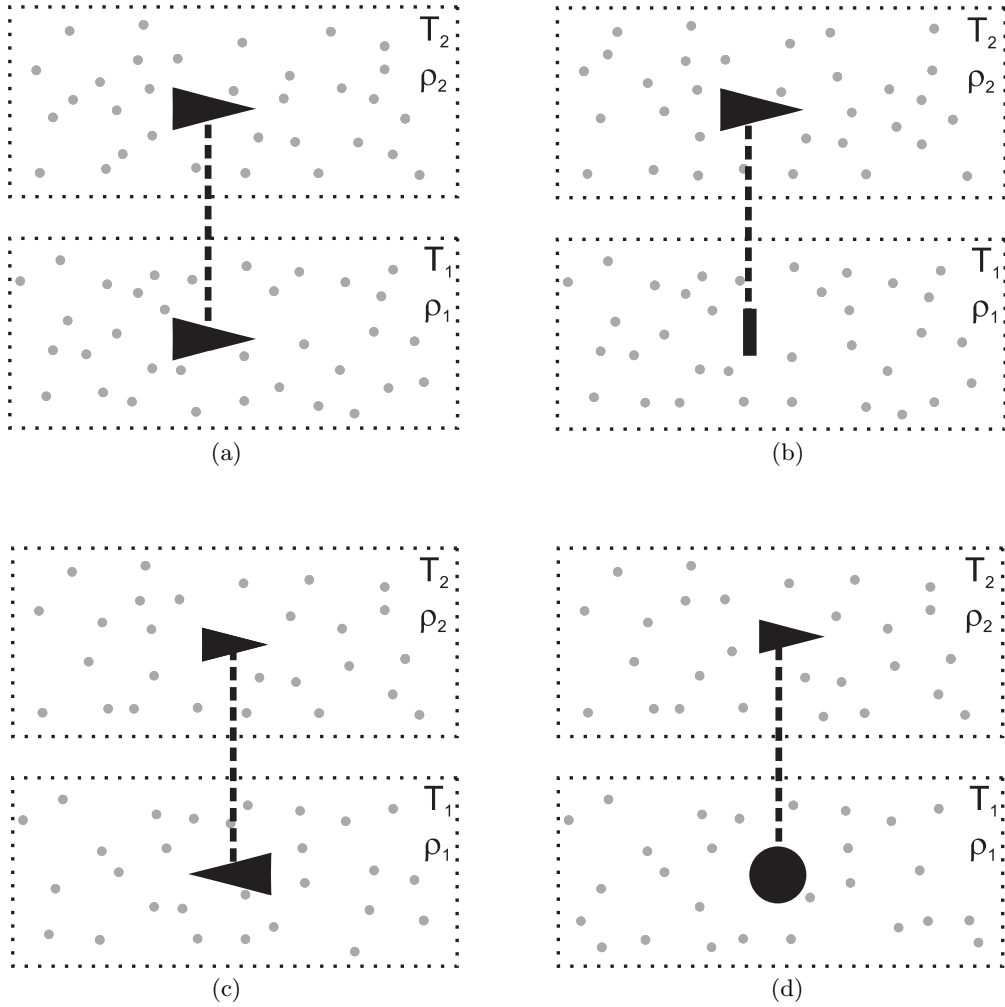


Figure 4: Four different realizations of the thermal Brownian motor, each consisting of two rigidly linked units. The units are simple convex objects: a bar of length L , a disk of radius R or an isosceles triangle with apex angle $2\theta_0$ and base L . (a) was introduced in [16] and will be referred to here as *Triangula*.

moment $A_n(x)$, cf. (7), is then:

$$\begin{aligned}
 A_n(x) = & (-1)^n 2^{(3n-1)/2} \sum_i S_i \rho_i \sqrt{\frac{k_B T_i}{\pi m}} \left(\frac{T_i}{T_{\text{eff}}}\right)^{n/2} \varepsilon^{-n/2} \\
 & \left(\int_{\sin \theta < 0} + (-1)^n \int_{\sin \theta > 0} \right) d\theta F_i(\theta) \exp \left[-\frac{T_{\text{eff}} \sin^2 \theta}{2T_i} x^2 \varepsilon^2 \right] \left(\frac{\varepsilon^2 \sin \theta}{1 + \varepsilon^2 \sin^2 \theta} \right)^n \\
 & \left(\Gamma \left[1 + \frac{n}{2} \right] \Phi \left[1 + \frac{n}{2}, \frac{1}{2}, \frac{T_{\text{eff}} \sin^2 \theta}{2T_i} x^2 \varepsilon^2 \right] + \varepsilon x \sin \theta \sqrt{\frac{2T_{\text{eff}}}{T_i}} \Gamma \left[\frac{3+n}{2} \right] \Phi \left[\frac{3+n}{2}, \frac{3}{2}, \frac{T_{\text{eff}} \sin^2 \theta}{2T_i} x^2 \varepsilon^2 \right] \right) \quad (31)
 \end{aligned}$$

with Γ the Gamma function (12) and Φ the Kummer function (13).

C. Stationary speed

The equations of moments (8), together with the explicit expressions for the jump moments (31), provide the starting point for a straightforward series expansion in terms of the small parameter ε . The equations for the first

and second moment, expanded up to order ε^5 and ε^4 respectively, are given by ($\tau = \varepsilon^2 t$):

$$\begin{aligned} \partial_\tau \langle x \rangle &= \sum_i S_i \rho_i \sqrt{\frac{k_B T_i}{m}} \left[-2 \sqrt{\frac{2}{\pi}} \langle \sin^2 \theta \rangle_i \langle x \rangle + \left(\sqrt{\frac{T_i}{T_{\text{eff}}}} - \sqrt{\frac{T_{\text{eff}}}{T_i}} \langle x^2 \rangle \right) \langle \sin^3 \theta \rangle_i \varepsilon \right. \\ &\quad + \frac{1}{3} \sqrt{\frac{2}{\pi}} \left(6 \langle x \rangle - \frac{T_{\text{eff}}}{T_i} \langle x^3 \rangle \right) \langle \sin^4 \theta \rangle_i \varepsilon^2 - \left(\sqrt{\frac{T_i}{T_{\text{eff}}}} - \sqrt{\frac{T_{\text{eff}}}{T_i}} \langle x^2 \rangle \right) \langle \sin^5 \theta \rangle_i \varepsilon^3 \\ &\quad \left. + \sqrt{\frac{2}{\pi}} \left(-2 \langle x \rangle + \frac{1}{3} \frac{T_{\text{eff}}}{T_i} \langle x^3 \rangle + \frac{1}{60} \left(\frac{T_{\text{eff}}}{T_i} \right)^2 \langle x^5 \rangle \right) \langle \sin^6 \theta \rangle_i \varepsilon^4 + \left(\sqrt{\frac{T_i}{T_{\text{eff}}}} - \sqrt{\frac{T_{\text{eff}}}{T_i}} \langle x^2 \rangle \right) \langle \sin^7 \theta \rangle_i \varepsilon^5 \right] \\ &\quad + O(\varepsilon^6) \end{aligned} \quad (32)$$

$$\begin{aligned} \partial_\tau \langle x^2 \rangle &= \sum_i S_i \rho_i \sqrt{\frac{k_B T_i}{m}} \left[-4 \sqrt{\frac{2}{\pi}} \left(-\frac{T_i}{T_{\text{eff}}} + \langle x^2 \rangle \right) \langle \sin^2 \theta \rangle_i + 2 \left(4 \sqrt{\frac{T_i}{T_{\text{eff}}}} \langle x \rangle - \sqrt{\frac{T_{\text{eff}}}{T_i}} \langle x^3 \rangle \right) \langle \sin^3 \theta \rangle_i \varepsilon \right. \\ &\quad + 2 \sqrt{\frac{2}{\pi}} \left(-4 \frac{T_i}{T_{\text{eff}}} + 5 \langle x^2 \rangle - \frac{1}{3} \frac{T_{\text{eff}}}{T_i} \langle x^4 \rangle \right) \langle \sin^4 \theta \rangle_i \varepsilon^2 + 2 \left(-7 \sqrt{\frac{T_i}{T_{\text{eff}}}} \langle x \rangle + 2 \sqrt{\frac{T_{\text{eff}}}{T_i}} \langle x^3 \rangle \right) \langle \sin^5 \theta \rangle_i \varepsilon^3 \\ &\quad \left. + \sqrt{\frac{2}{\pi}} \left(-16 \langle x^2 \rangle + \frac{7}{6} \frac{T_{\text{eff}}}{T_i} \langle x^4 \rangle + \frac{1}{30} \left(\frac{T_{\text{eff}}}{T_i} \right)^2 \langle x^6 \rangle \right) \langle \sin^6 \theta \rangle_i \varepsilon^4 \right] + O(\varepsilon^5). \end{aligned} \quad (33)$$

Note that a term of order ε^{-1} in the series for $\partial_\tau \langle x \rangle$ is zero because of the property (22.c). Such a term would correspond to a constant, velocity-independent, force acting on the object. It should indeed be zero, since each gas mixture separately is in equilibrium. From Eq. (32) we also immediately recognize to lowest order in ε the linear relaxation law, written in original variables as $M \partial_t \langle V \rangle = -\gamma V$, with $\gamma = \sum_i \gamma_i$ and γ_i the linear friction coefficient, due to the section of the motor sitting in gas mixture i :

$$\gamma_i = 4 S_i \rho_i \sqrt{\frac{k_B T_i m}{2\pi}} \int_0^{2\pi} d\theta F_i(\theta) \sin^2 \theta. \quad (34)$$

At this level of the perturbation, the speed of the object is zero: no rectification takes place at the level of linear response.

In order to find the first non-zero contribution to the velocity $\langle x \rangle$, we need the terms up to order ε . From the definition of T_{eff} , by the condition $\langle x^2 \rangle = 1$ up to lowest order in ε , we find from Eq. (33):

$$T_{\text{eff}} = \frac{\sum_i \gamma_i T_i}{\sum_i \gamma_i}. \quad (35)$$

The lowest non-zero term for the average velocity then follows from Eq. (32) and reads in the original variable V :

$$\langle V \rangle = \sqrt{\frac{m}{M}} \sqrt{\frac{\pi k_B T_{\text{eff}}}{8M}} \frac{\sum_i S_i \rho_i \left(\frac{T_i}{T_{\text{eff}}} - 1 \right) \int_0^{2\pi} d\theta F_i(\theta) \sin^3 \theta}{\sum_i S_i \rho_i \sqrt{\frac{T_i}{T_{\text{eff}}}} \int_0^{2\pi} d\theta F_i(\theta) \sin^2(\theta)} + \dots \quad (36)$$

This speed is equal to the expansion parameter times the thermal speed of the motor and further multiplied by a factor that depends on the geometric properties of the object. Note that the Brownian motor ceases to function in the absence of a temperature difference (when $T_i = T_{\text{eff}}$ for all i) and in the macroscopic limit $M \rightarrow \infty$ (since $\langle V \rangle \sim 1/M$). Note also that the speed is scale-independent, i.e., independent of the actual size of the motor units: $\langle V \rangle$ is invariant under the rescaling S_i to $C S_i$. To isolate more clearly the effect of the asymmetry of the motor on its speed, we focus on the case where the units have the same shape in all compartments, i.e. $F_i(\theta) \equiv F(\theta)$ and $S_i \equiv S$. One finds:

$$T_{\text{eff}} = \frac{\sum_i \rho_i T_i^{3/2}}{\sum_i \rho_i \sqrt{T_i}}, \quad (37)$$

and

$$\langle V \rangle = \sqrt{\frac{m}{M}} \sqrt{\frac{\pi k_B T_{\text{eff}}}{8M}} \frac{\sum_i \rho_i \left(\frac{T_i}{T_{\text{eff}}} - 1 \right) \langle \sin^3 \theta \rangle}{\sum_i \rho_i \sqrt{\frac{T_i}{T_{\text{eff}}}} \langle \sin^2 \theta \rangle} + \dots \quad (38)$$

Shape	Circumference S	Form factor $F(\theta)$	Friction coefficient γ
Bar	$2L$	$\frac{1}{2} (\delta [\theta - \frac{\pi}{2}] + \delta [\theta - \frac{3\pi}{2}])$	$8L\rho\sqrt{\frac{k_B T m}{2\pi}}$
Disk	$2\pi R$	$1/2\pi$	$4\pi R\rho\sqrt{\frac{k_B T m}{2\pi}}$
Triangle	$L \frac{1+\sin\theta_0}{\sin\theta_0}$	$\frac{2\delta[\theta - \frac{3\pi}{2}] \sin\theta_0 + \delta[\theta - \theta_0] + \delta[\theta - (\pi - \theta_0)]}{2(1+\sin\theta_0)}$	$4L\rho\sqrt{\frac{k_B T m}{2\pi}}(1 + \sin\theta_0)$

Table I: The circumference S , the form factor $F(\theta)$ and the friction coefficient γ in a gas with density ρ and temperature T , for a vertical bar of length L , a disk with radius R and an isosceles triangle with base L and apex angle $2\theta_0$, pointed in the x -direction.

In this case T_{eff} is independent of $F(\theta)$ and the drift velocity is proportional to $\langle \sin^3 \theta \rangle / \langle \sin^2 \theta \rangle$, with the average defined with respect to $F(\theta)$. The latter ratio is in absolute value always smaller than 1, a value that can be reached for “strongly” asymmetric objects as will be shown below on specific examples. The resulting speed is then very large, i.e., comparable to the thermal speed.

Calculation of the average speed up to order ε^5 requires the evaluation of $\langle x^2 \rangle$, $\langle x^3 \rangle$, $\langle x^4 \rangle$, $\langle x^5 \rangle$ and $\langle x^6 \rangle$, up to orders ε^4 , ε^3 , ε^2 , ε and ε^0 respectively, cf. appendix B. This calculation has been carried out using symbolic manipulations, and the resulting expressions have been used in Table IV and Fig. 5. However, since the analytic expressions are very involved, we only reproduce the result here up to order ε^3 :

$$\begin{aligned}
\langle V \rangle = & \sqrt{\frac{m}{M}} \sqrt{\frac{\pi k_B T_{\text{eff}}}{8M}} \frac{\sum_i S_i \rho_i \left(\frac{T_i}{T_{\text{eff}}} - 1 \right) \langle \sin^3 \theta \rangle_i}{\sum_i S_i \rho_i \sqrt{\frac{T_i}{T_{\text{eff}}}} \langle \sin^2 \theta \rangle_i} \\
& + \left(\frac{m}{M} \right)^{3/2} \sqrt{\frac{\pi k_B T_{\text{eff}}}{8M}} \left\{ \frac{\sum_i S_i \rho_i \left(1 - \frac{T_i}{T_{\text{eff}}} \right) \langle \sin^5 \theta \rangle_i}{\sum_i S_i \rho_i \sqrt{\frac{T_i}{T_{\text{eff}}}} \langle \sin^2 \theta \rangle_i} \right. \\
& + \frac{\left(\sum_i S_i \rho_i \sqrt{\frac{T_i}{T_{\text{eff}}}} \langle \sin^4 \theta \rangle_i \right) \left(\sum_i S_i \rho_i \left(\frac{T_i}{T_{\text{eff}}} - \frac{7}{2} \right) \langle \sin^3 \theta \rangle_i \right)}{\left[\sum_i S_i \rho_i \sqrt{\frac{T_i}{T_{\text{eff}}}} \langle \sin^2 \theta \rangle_i \right]^2} \\
& + \frac{\sum_i S_i \rho_i \langle \sin^3 \theta \rangle_i}{\sum_i S_i \rho_i \sqrt{\frac{T_i}{T_{\text{eff}}}} \langle \sin^2 \theta \rangle_i} \left[\frac{\sum_i S_i \rho_i \left(2 \left(\frac{T_i}{T_{\text{eff}}} \right)^{3/2} + \frac{1}{2} \sqrt{\frac{T_i}{T_{\text{eff}}}} \right) \langle \sin^4 \theta \rangle_i}{\sum_i S_i \rho_i \sqrt{\frac{T_i}{T_{\text{eff}}}} \langle \sin^2 \theta \rangle_i} \right. \\
& \left. \left. - \frac{\pi \left(\sum_i S_i \rho_i \frac{T_i}{T_{\text{eff}}} \langle \sin^3 \theta \rangle_i \right) \left(\sum_i S_i \rho_i \left(\frac{T_i}{T_{\text{eff}}} - 1 \right) \langle \sin^3 \theta \rangle_i \right)}{2 \left[\sum_i S_i \rho_i \sqrt{\frac{T_i}{T_{\text{eff}}}} \langle \sin^2 \theta \rangle_i \right]^2} \right] \right. \\
& \left. + \left[\frac{\pi}{4} \left(\frac{\sum_i S_i \rho_i \langle \sin^3 \theta \rangle_i}{\sum_i S_i \rho_i \sqrt{\frac{T_i}{T_{\text{eff}}}} \langle \sin^2 \theta \rangle_i} \right)^2 - \frac{1}{3} \frac{\sum_i S_i \rho_i \sqrt{\frac{T_i}{T_{\text{eff}}}} \langle \sin^4 \theta \rangle_i}{\sum_i S_i \rho_i \sqrt{\frac{T_i}{T_{\text{eff}}}} \langle \sin^2 \theta \rangle_i} \right] \left[\frac{\sum_i S_i \rho_i \left(-2 \left(\frac{T_i}{T_{\text{eff}}} \right)^2 + \frac{9}{2} \frac{T_i}{T_{\text{eff}}} - \frac{5}{2} \right) \langle \sin^3 \theta \rangle_i}{\sum_i S_i \rho_i \sqrt{\frac{T_i}{T_{\text{eff}}}} \langle \sin^2 \theta \rangle_i} \right] \right\} \\
& + \dots
\end{aligned} \tag{39}$$

D. Special cases

The above analytic result, Eq. (39), is valid for any convex shape of the constituting pieces. To illustrate the type of explicit results that are obtained, we focus on simple shapes like a disk, a bar and a triangle. In Table I the circumference S , the form factor $F(\theta)$ and the friction coefficient γ are calculated for these objects. Note that the

Shape	Figure	Stationary velocity $\langle V \rangle$ (order ε)
Triangula	Fig. 4a.	$\frac{\sqrt{2\pi k_B m}}{4M} (1 - \sin \theta_0) \frac{\rho_1 \rho_2 (T_1 - T_2) (\sqrt{T_1} - \sqrt{T_2})}{[\rho_1 \sqrt{T_1} + \rho_2 \sqrt{T_2}]^2}$
Triangle - bar	Fig. 4b.	$\frac{\sqrt{2\pi k_B m}}{4M} (1 - \sin^2 \theta_0) \frac{2\rho_1 \rho_2 \sqrt{T_1} (T_1 - T_2)}{[2\rho_1 \sqrt{T_1} + \rho_2 \sqrt{T_2} (1 + \sin \theta_0)]^2}$
Triangle - triangle	Fig. 4c.	$\frac{\sqrt{2\pi k_B m}}{4M} (1 - \sin \theta_0) \frac{\rho_1 \rho_2 (T_1 - T_2) (\sqrt{T_1} + \sqrt{T_2})}{[\rho_1 \sqrt{T_1} + \rho_2 \sqrt{T_2}]^2}$
Triangle - disk	Fig. 4d.	$\frac{\sqrt{2\pi k_B m}}{4M} (1 - \sin^2 \theta_0) \frac{\pi R}{L} \frac{\rho_1 \rho_2 \sqrt{T_1} (T_1 - T_2)}{[\frac{\pi R}{L} \rho_1 \sqrt{T_1} + (1 + \sin \theta_0) \rho_2 \sqrt{T_2}]^2}$

Table II: Analytic result for the lowest order contribution to $\langle V \rangle$ for the different constructions depicted in Fig. 4.

friction coefficient of the bar is in agreement with the result of the adiabatic piston problem, cf. Eq. (18).

A thermal Brownian motor can only operate under nonequilibrium conditions, which can be achieved if at least two of such units are each located in a reservoir containing an ideal gas at a different temperature. The two units are rigidly linked and can move as a single degree of freedom along the x -direction. Besides the nonequilibrium constraint, a spatial asymmetry is also required to yield a net motion. In particular, a construction with only bars and/or disks will not generate any net motion. One of the simplest motors one can imagine was introduced in [16] and will be referred to as *Triangula*, see figure 4a. Two identical rigidly linked isosceles triangles (with apex angle $2\theta_0$, pointing in the x -direction) are each located in a reservoir containing a gas separately in equilibrium at a different temperature. The lowest order contribution to the average velocity of *Triangula* follows from Eq. (36), cf. Table I:

$$\langle V \rangle_{\text{Triangula}} = \frac{\sqrt{2\pi k_B m}}{4M} (1 - \sin \theta_0) \frac{\rho_1 \rho_2 (T_1 - T_2) (\sqrt{T_1} - \sqrt{T_2})}{[\rho_1 \sqrt{T_1} + \rho_2 \sqrt{T_2}]^2}. \quad (40)$$

The fact that the combination of the asymmetry and the temperature gradient is necessary to generate the systematic motion, is contained in Eq. (40). If either $T_1 = T_2$ or $\theta_0 = \pi/2$ (the triangle becomes a bar and thus the asymmetry disappears), the average velocity vanishes. The corrections of order ε^3 to this formula can be found in appendix B. The dependence of the speed on the temperatures and densities are reproduced in Fig. 5. Note that from Eq. (40) may be concluded that the speed of *Triangula* is maximal for $\rho_1 \sqrt{T_1} = \rho_2 \sqrt{T_2}$. Fig. 4 also shows some other variations of the thermal Brownian motor. Their drift speed up to lowest order in ε can be found in Table II. One can easily verify that each thermal Brownian motor ceases to function when the spatial asymmetry or the temperature difference vanish. In this context it is sometimes stated that equilibrium is a point of flux reversal. This is indeed the case for our microscopic model except when there are special symmetries in the system. When the units in the two reservoirs are not the same, the direction of the net motion changes when the temperature difference changes sign. From the models depicted in Fig. 4, only *Triangula* keeps its original direction of motion. In this latter case, the speed exhibits a parabolic minimum as a function of the temperature, with zero speed at equilibrium. The reason for this peculiar behavior derives from the permutational symmetry of identical units, implying that the speed must be invariant under the interchange of T_1, ρ_1 with T_2, ρ_2 . In particular it must be an even function of $T_1 - T_2$ when $\rho_1 = \rho_2$.

V. COMPARISON WITH SIMULATIONS

The analytic results for the adiabatic piston and the thermal Brownian motor are compared with the results of the numerical solution of the Boltzmann equation in Table III and Table IV respectively. To improve the precision of these simulations, we used a special technique for solving a Master equation, based on the introduction of a simple envelope process, see appendix C for details. The agreement between theory and simulations is very satisfactory, and only breaks down, as expected, for small ratios m/M where the perturbative result becomes inaccurate. We have also included for completeness the results obtained by molecular dynamics simulations, cf. [16] for more details. We used low densities for the hard disks, $\rho = .0022$, a regime in which one comes close to the properties of an ideal gas. Nevertheless one expects strong finite size effects, due to the fact that the reservoirs containing the gases are not very large. To cite just one important phenomenon, we note that the motion of the motor will generate sound waves

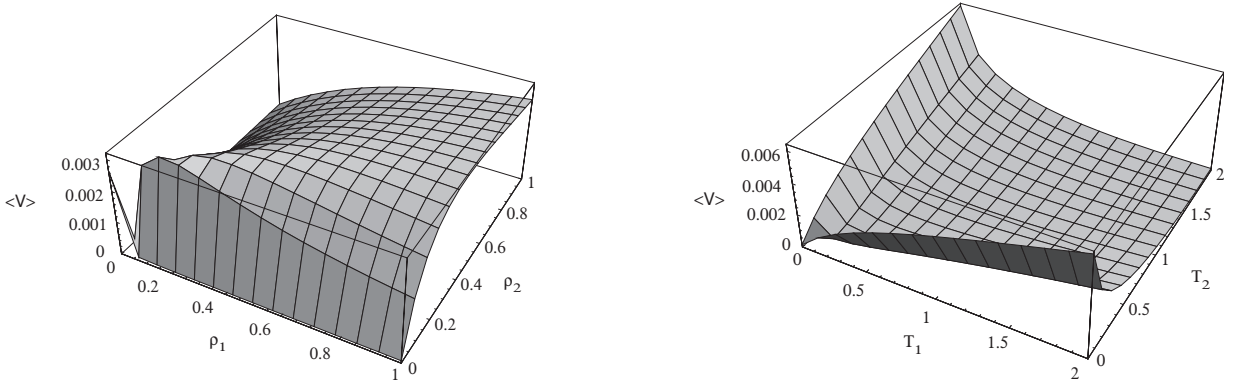


Figure 5: Average speed of Triangula according to Eq. (B4). Left: the dependence of the velocity on the densities ($T_1 = 1.0$ and $T_2 = 5.0$). Right: The stationary speed increases with the temperature difference ($\rho_1 = \rho_2 = 0.0022$). The following parameter values were used: mass of the gas particles $m = 1$, total mass of the motor $M = 100$, apex angle of the triangles $2\theta_0 = \pi/18$ and $k_B = 1$ by choice of units.

Mass M	Theory (order ε)	Theory (order $\varepsilon + \varepsilon^3$)	Theory (order $\varepsilon + \varepsilon^3 + \varepsilon^5$)	Boltzmann equation
1	5.64	-7.82	20.44	1.411
5	1.13	0.590	0.8158	0.7289
20	0.282	0.2484	0.2519	0.2511
50	0.113	0.1074	0.1076	0.1076
100	0.0564	0.05505	0.05508	0.0554
200	0.0282	0.02786	0.02787	0.0280

Table III: Stationary average speed of the *adiabatic piston* from the perturbative solution method up to order ε , ε^3 and ε^5 , compared with the result from a numerical solution of the Boltzmann equation. The following parameter values were used: particle densities $\rho_1 = 10^{-2}$ and $\rho_2 = 1$, temperatures $T_1 = 100$ and $T_2 = 1$ and mass of the gas particles $m = 1$. $k_B = 1$ by choice of units.

that will reimpact on it. Taking this into account, the speeds observed in the molecular dynamics are in reasonable agreement with the theoretical and numerical results obtained from the Boltzmann equation. Notably the speed of the thermal motor in the hard disk gases is systematically larger by roughly 20 to 40%, for reasons that are unclear to us.

Mass M	Theory (order ε)	Theory (order $\varepsilon + \varepsilon^3$)	Theory (order $\varepsilon + \varepsilon^3 + \varepsilon^5$)	Boltzmann equation	Molecular Dynamics
1	0.38	-1.23	11.66	0.057	0.12
5	0.076	0.01188	0.1150	0.0470	0.064
20	0.0190	0.01502	0.01663	0.0157	0.024
50	0.00762	0.006974	0.007077	0.0071	0.0093
100	0.00381	0.003648	0.003661	0.0035	0.0043
200	0.00190	0.001864	0.001866	0.0017	0.0021

Table IV: Stationary average speed of the thermal Brownian motor *Triangula* from the perturbative solution method up to order ε , ε^3 and ε^5 , compared with the result from a numerical solution of the Boltzmann equation. The following parameter values were used: particle densities $\rho_1 = \rho_2 = 0.00222$, temperatures $T_1 = 1.9$ and $T_2 = 0.1$, mass of the particles $m = 1$ and apex angle of the triangle $2\theta_0 = \pi/18$. $k_B = 1$ by choice of units. For comparison, we also include the speed observed in molecular dynamics, see [16] for more details.

VI. DISCUSSION

The problem of the Maxwell demon has been haunting the imagination and theoretical efforts of physicists for more than hundred years. While there is a consensus that one cannot rectify fluctuations at equilibrium, it is recomforting that one can construct microscopic models, involving interactions with ideal gases only, for which this thesis can be verified explicitly. The same models can be used as test cases for another important field of interest, namely the rectification of thermal fluctuations in nonequilibrium, also referred to as Brownian motors. In this respect we claim that our model is a genuine Brownian motor: the rectification appears at the level of nonlinear response, where the usual separation between systematic and noise terms, as made explicit in a linear Langevin equation, is no longer possible. Hence the operation of our Brownian motor falls outside the scope of linear irreversible thermodynamics. It belongs to the realm of microscopic theory in which nonlinearity and noise form an intertwined part of the microscopic dynamics. This is in contrast to most of the Brownian motors discussed with mesoscopic theory. For example, the prototype model of one class of Brownian motors referred to as flashing ratchet can be described by diffusion in an external potential, a standard problem in linear irreversible thermodynamics.

Appendix A: DETAILS ON THE CALCULATION FOR THE ADIABATIC PISTON

Expansion of the rescaled jump moments $A_n(x)$ (11) in the moment equations (8) yields the following power series expansion in $\varepsilon = \sqrt{m/M}$, with the first and second moment expanded up to fifth and fourth order in ε (cf. Eqs. (16-17)) respectively, and the higher moments $\langle x^3 \rangle, \langle x^4 \rangle, \langle x^5 \rangle$ and $\langle x^6 \rangle$ up to $\varepsilon^3, \varepsilon^2, \varepsilon$ and ε^0 respectively:

$$\begin{aligned}
 \partial_\tau \langle x^3 \rangle &= 6 (2 f[3/2] \langle x \rangle - f[1/2] \langle x^3 \rangle) - 3 (4 g[2] + g[0] \langle x^4 \rangle) \varepsilon \\
 &\quad + (-56 f[3/2] \langle x \rangle + 24 f[1/2] \langle x^3 \rangle - f[-1/2] \langle x^5 \rangle) \varepsilon^2 + 9 (4 g[2] + g[0] \langle x^4 \rangle) \varepsilon^3 + O(\varepsilon^4) \\
 \partial_\tau \langle x^4 \rangle &= 8 (3 f[3/2] \langle x^2 \rangle - f[1/2] \langle x^4 \rangle) - 4 (12 g[2] \langle x \rangle + g[0] \langle x^5 \rangle) \varepsilon \\
 &\quad + 4 \left(16 f[5/2] - 44 f[3/2] \langle x^2 \rangle + 11 f[1/2] \langle x^4 \rangle - \frac{1}{3} f[-1/2] \langle x^6 \rangle \right) \varepsilon^2 + O(\varepsilon^3) \\
 \partial_\tau \langle x^5 \rangle &= 10 (4 f[3/2] \langle x^3 \rangle - f[1/2] \langle x^5 \rangle) - 5 (24 g[2] \langle x^2 \rangle + g[0] \langle x^6 \rangle) \varepsilon + O(\varepsilon^2) \\
 \partial_\tau \langle x^6 \rangle &= 12 (5 f[3/2] \langle x^4 \rangle - f[1/2] \langle x^6 \rangle) + O(\varepsilon).
 \end{aligned} \tag{A1}$$

In the stationary regime these equations form, together with Eqs. (16-17), an algebraic set of equations, which can be solved to find the stationary average velocity $\langle x \rangle$ up to order ε^5 . The result in terms of the original variable

$V = \sqrt{\frac{k_B T_{\text{eff}}}{M}} x$ is given in Eq. (21). The corresponding results for the higher order moments read:

$$\begin{aligned}
\langle V^2 \rangle &= \frac{k_B \sqrt{T_1 T_2}}{M} \\
&+ \frac{k_B m}{M^2} \left(\frac{\sqrt{T_1 T_2}}{2} + \frac{\pi}{8} (\sqrt{T_1} - \sqrt{T_2})^2 - \frac{1}{2} \frac{(\rho_1 T_1^{-1/2} + \rho_2 T_2^{-1/2}) T_1 T_2}{\rho_1 \sqrt{T_1} + \rho_2 \sqrt{T_2}} \right) \\
&+ \frac{k_B m^2}{M^3} \left(\frac{\sqrt{T_1 T_2}}{4} - \frac{2}{3} \frac{(\rho_1 T_1^{-1/2} + \rho_2 T_2^{-1/2})^2 (T_1 T_2)^{3/2}}{(\rho_1 \sqrt{T_1} + \rho_2 \sqrt{T_2})^2} \right. \\
&\quad \left. - \frac{29\pi}{48} (\sqrt{T_1} - \sqrt{T_2})^2 - \frac{3\pi^2}{16} \frac{(\sqrt{T_1} - \sqrt{T_2})^4}{\sqrt{T_1 T_2}} + \frac{35\pi}{48} \frac{\rho_1 T_1^{5/2} + \rho_2 T_2^{5/2}}{\rho_1 \sqrt{T_1} + \rho_2 \sqrt{T_2}} \frac{(\sqrt{T_1} - \sqrt{T_2})^2}{T_1 T_2} \right. \\
&\quad \left. + \frac{1}{8} \frac{(\rho_1 T_1^{-3/2} + \rho_2 T_2^{-3/2}) (T_1 T_2)^{3/2}}{\rho_1 \sqrt{T_1} + \rho_2 \sqrt{T_2}} + \frac{7}{24} \frac{(\rho_1 T_1^{-1/2} + \rho_2 T_2^{-1/2}) T_1 T_2}{\rho_1 \sqrt{T_1} + \rho_2 \sqrt{T_2}} \right) + \dots \\
\langle V^3 \rangle &= \frac{\sqrt{k_B^3 m \pi}}{2\sqrt{2} M^2} (\sqrt{T_1} - \sqrt{T_2}) \sqrt{T_1 T_2} \\
&+ \frac{\sqrt{k_B^3 m^3 \pi}}{\sqrt{2} M^3} \left(-\frac{8}{3} (\sqrt{T_1} - \sqrt{T_2}) \sqrt{T_1 T_2} - \frac{3\pi}{4} (\sqrt{T_1} - \sqrt{T_2})^3 + \frac{7}{4} \frac{(\sqrt{T_1} - \sqrt{T_2}) (\rho_1 T_1^{5/2} + \rho_2 T_2^{5/2})}{(\rho_1 \sqrt{T_1} + \rho_2 \sqrt{T_2}) \sqrt{T_1 T_2}} \right) + \dots \\
\langle V^4 \rangle &= 3 \left(\frac{k_B \sqrt{T_1 T_2}}{M} \right)^2 + \frac{k_B^2 m}{M^3} \left(-4 T_1 T_2 - \frac{7\pi}{4} (\sqrt{T_1} - \sqrt{T_2})^2 \sqrt{T_1 T_2} + 4 \frac{\rho_1 T_1^{5/2} + \rho_2 T_2^{5/2}}{\rho_1 \sqrt{T_1} + \rho_2 \sqrt{T_2}} \right) + \dots \\
\langle V^5 \rangle &= -\frac{\sqrt{k_B^5 m \pi}}{M^3} \frac{5}{2\sqrt{2}} (\sqrt{T_1} - \sqrt{T_2}) T_1 T_2 + \dots \\
\langle V^6 \rangle &= 15 \left(\frac{k_B \sqrt{T_1 T_2}}{M} \right)^3 + \dots \tag{A2}
\end{aligned}$$

Note that the lowest order terms are consistent with the observation that the velocity distribution itself is Gaussian at the lowest order, cf. [14].

Appendix B: DETAILS ON THE CALCULATION FOR A THERMAL BROWNIAN MOTOR OF A GENERAL SHAPE

A perturbative series in ε for the moments, obtained by the expansion of Eqs. (8), together with the jump moments defined in (11). The resulting expressions for the first and second moment up to order ε^5 and ε^4 respectively are given in Eqs. (32-33). Calculation of $\langle V \rangle$ up to ε^5 requires furthermore $\langle x^3 \rangle$, $\langle x^4 \rangle$, $\langle x^5 \rangle$ and $\langle x^6 \rangle$ up to order ε^3 , ε^2 , ε and

ε^0 respectively:

$$\begin{aligned}
\partial_\tau \langle x^3 \rangle &= \sum_i S_i \rho_i \sqrt{\frac{k_B T_i}{m}} \left\{ 6 \sqrt{\frac{2}{\pi}} \left(2 \frac{T_i}{T_{\text{eff}}} \langle x \rangle - \langle x^3 \rangle \right) \langle \sin^2 \theta \rangle_i \right. \\
&\quad + 3 \left(-4 \left(\frac{T_i}{T_{\text{eff}}} \right)^{3/2} + 7 \sqrt{\frac{T_i}{T_{\text{eff}}}} \langle x^2 \rangle - \sqrt{\frac{T_{\text{eff}}}{T_i}} \langle x^4 \rangle \right) \langle \sin^3 \theta \rangle_i \varepsilon \\
&\quad + \sqrt{\frac{2}{\pi}} \left(-56 \frac{T_i}{T_{\text{eff}}} \langle x \rangle + 24 \langle x^3 \rangle - \frac{T_{\text{eff}}}{T_i} \langle x^5 \rangle \right) \langle \sin^4 \theta \rangle_i \varepsilon^2 \\
&\quad \left. + 3 \left(12 \left(\frac{T_i}{T_{\text{eff}}} \right)^{3/2} - 21 \sqrt{\frac{T_i}{T_{\text{eff}}}} \langle x^2 \rangle + 3 \sqrt{\frac{T_{\text{eff}}}{T_i}} \langle x^4 \rangle \right) \langle \sin^5 \theta \rangle_i \varepsilon^3 \right\} + O(\varepsilon^4) \\
\partial_\tau \langle x^4 \rangle &= 4 \sum_i S_i \rho_i \sqrt{\frac{k_B T_i}{m}} \left\{ 2 \sqrt{\frac{2}{\pi}} \left(3 \frac{T_i}{T_{\text{eff}}} \langle x^2 \rangle - \langle x^4 \rangle \right) \langle \sin^2 \theta \rangle_i \right. \\
&\quad + \left(-12 \left(\frac{T_i}{T_{\text{eff}}} \right)^{3/2} \langle x \rangle + 10 \sqrt{\frac{T_i}{T_{\text{eff}}}} \langle x^3 \rangle - \sqrt{\frac{T_{\text{eff}}}{T_i}} \langle x^5 \rangle \right) \langle \sin^3 \theta \rangle_i \varepsilon \\
&\quad \left. + \sqrt{\frac{2}{\pi}} \left(16 \left(\frac{T_i}{T_{\text{eff}}} \right)^2 - 44 \frac{T_i}{T_{\text{eff}}} \langle x^2 \rangle + 11 \langle x^4 \rangle - \frac{1}{3} \frac{T_{\text{eff}}}{T_i} \langle x^6 \rangle \right) \langle \sin^4 \theta \rangle_i \varepsilon^2 \right\} + O(\varepsilon^3) \\
\partial_\tau \langle x^5 \rangle &= 5 \sum_i S_i \rho_i \sqrt{\frac{k_B T_i}{m}} \left\{ 2 \sqrt{\frac{2}{\pi}} \left(4 \frac{T_i}{T_{\text{eff}}} \langle x^3 \rangle - \langle x^5 \rangle \right) \langle \sin^2 \theta \rangle_i \right. \\
&\quad \left. + \left(-24 \left(\frac{T_i}{T_{\text{eff}}} \right)^{3/2} \langle x^2 \rangle + 13 \sqrt{\frac{T_i}{T_{\text{eff}}}} \langle x^4 \rangle - \sqrt{\frac{T_{\text{eff}}}{T_i}} \langle x^6 \rangle \right) \langle \sin^3 \theta \rangle_i \varepsilon \right\} + O(\varepsilon^2) \\
\partial_\tau \langle x^6 \rangle &= 12 \sum_i S_i \rho_i \sqrt{\frac{k_B T_i}{m}} \left\{ \sqrt{\frac{2}{\pi}} \left(5 \frac{T_i}{T_{\text{eff}}} \langle x^4 \rangle - \langle x^6 \rangle \right) \langle \sin^2 \theta \rangle_i \right\} + O(\varepsilon) \tag{B1}
\end{aligned}$$

In the stationary regime, these equations form together with Eqs. (32-33) an algebraic set of equations from which the average velocity can be obtained up to order ε^5 . The analytical expression in the original variable V up to ε^3 is reproduced in Eq. (39). The corresponding power series for the higher moments of the stationary velocity distribution function are:

$$\begin{aligned}
\langle V^2 \rangle &= \frac{k_B T_{\text{eff}}}{M} + \frac{k_B m T_{\text{eff}}}{M^2} \left\{ \frac{\sum_i S_i \rho_i \left(-2 \left(\frac{T_i}{T_{\text{eff}}} \right)^{3/2} + \frac{5}{2} \sqrt{\frac{T_i}{T_{\text{eff}}}} - \frac{1}{2} \sqrt{\frac{T_{\text{eff}}}{T_i}} \right) \langle \sin^4 \theta \rangle_i}{\sum_i S_i \rho_i \sqrt{\frac{T_i}{T_{\text{eff}}}} \langle \sin^2 \theta \rangle_i} \right. \\
&\quad \left. - \frac{\pi}{4} \frac{(\sum_i S_i \rho_i \langle \sin^3 \theta \rangle_i) \left(\sum_i S_i \rho_i \left(-2 \left(\frac{T_i}{T_{\text{eff}}} \right)^2 + \frac{13}{2} \frac{T_i}{T_{\text{eff}}} - \frac{5}{2} \right) \langle \sin^3 \theta \rangle_i \right) - 2 \left(\sum_i S_i \rho_i \frac{T_i}{T_{\text{eff}}} \langle \sin^3 \theta \rangle_i \right)^2}{\left[\sum_i S_i \rho_i \sqrt{\frac{T_i}{T_{\text{eff}}}} \langle \sin^2 \theta \rangle_i \right]^2} \right\} + \dots \\
\langle V^3 \rangle &= \sqrt{\frac{m}{M}} \left(\frac{k_B T_{\text{eff}}}{M} \right)^{3/2} \left[\sqrt{\frac{\pi}{2}} \frac{\sum_i S_i \rho_i \left(-2 \left(\frac{T_i}{T_{\text{eff}}} \right)^2 + \frac{9}{2} \frac{T_i}{T_{\text{eff}}} - \frac{5}{2} \right) \langle \sin^3 \theta \rangle_i}{\sum_i S_i \rho_i \sqrt{\frac{T_i}{T_{\text{eff}}}} \langle \sin^2 \theta \rangle_i} \right] + \dots \\
\langle V^4 \rangle &= 3 \left(\frac{k_B T_{\text{eff}}}{M} \right)^2 + \dots \\
\langle V^5 \rangle &= \sqrt{\frac{m}{M}} \left(\frac{k_B T_{\text{eff}}}{M} \right)^{5/2} \left[\sqrt{\frac{\pi}{2}} \frac{\sum_i S_i \rho_i \left(-20 \left(\frac{T_i}{T_{\text{eff}}} \right)^2 + \frac{75}{2} \frac{T_i}{T_{\text{eff}}} - \frac{35}{2} \right) \langle \sin^3 \theta \rangle_i}{\sum_i S_i \rho_i \sqrt{\frac{T_i}{T_{\text{eff}}}} \langle \sin^2 \theta \rangle_i} \right] + \dots \\
\langle V^6 \rangle &= 15 \left(\frac{k_B T_{\text{eff}}}{M} \right)^3 + \dots \tag{B2}
\end{aligned}$$

For the particular case of Triangula, see Fig. 4a., one can verify that

$$T_{\text{eff}} = \frac{\rho_1 T_1^{3/2} + \rho_2 T_2^{3/2}}{\rho_1 \sqrt{T_1} + \rho_2 \sqrt{T_2}}$$

$$\langle \sin^n \theta \rangle = \frac{(-1)^n \sin \theta_0 + \sin^n \theta_0}{1 + \sin \theta_0} \quad (\text{B3})$$

The average speed of Triangula up to ε^3 reads:

$$\langle V \rangle = \sqrt{\frac{m}{M}} \sqrt{\frac{\pi k_B T_{\text{eff}}}{2M}} \frac{1}{2} (h[1] - h[0]) (\sin \theta_0 - 1)$$

$$\left(\frac{m}{M}\right)^{3/2} \sqrt{\frac{\pi k_B T_{\text{eff}}}{2M}} \left\{ \frac{1}{2} (h[0] - h[1]) \frac{\sin^4 \theta_0 - 1}{\sin \theta_0 + 1} + \frac{\pi h[0]}{4} \left(-h[1]^2 - h[0]h[2] + \frac{13}{4}h[0]h[1] - \frac{5}{4}h[0]^2 \right) (\sin \theta_0 - 1)^3 \right.$$

$$+ \left(\frac{1}{2}h[1/2]h[1] - \frac{7}{4}h[1/2]h[0] + h[0]h[3/2] + \frac{1}{3}h[-1/2]h[2] - \frac{3}{4}h[-1/2]h[1] + \frac{2}{3}h[-1/2]h[0] \right)$$

$$\left. \times \frac{(\sin \theta_0 - 1)(1 + \sin^3 \theta_0)}{1 + \sin \theta_0} \right\}, \quad (\text{B4})$$

with

$$h[n] = \frac{\rho_1 T_1^n + \rho_2 T_2^n}{\rho_1 \sqrt{T_1} + \rho_2 \sqrt{T_2}} T_{\text{eff}}^{-n+1/2}. \quad (\text{B5})$$

Appendix C: SIMULATION OF THE MASTER EQUATION

Consider a Markov process, defined by the transition rate $W(V|V')$, for transitions from state V' to V . We decompose the transition rate as follows

$$W(V|V') = R(V')P(V|V')$$

where $R(V') = \int dV W(V|V')$ is the total rate and $P(V|V')$ is the conditional probability. Stochastic trajectories of V may be easily produced if the probability P can be easily realized, that is, if it is simple to generate random values with that distribution. However, for complicated W and P this direct approach is often not possible and an alternative construction is necessary.

We introduce an “envelope” process, $W^*(V|V')$, for which $W^* \geq W$ for all V, V' , cf. [19]. The difference

$$W_0(V') = W^*(V|V') - W(V|V')$$

is called the “null” process. The envelope process is chosen such that R^* is a constant and that P^* has a simple form (e.g., a Gaussian distribution).

The simulation of trajectories of W then proceeds as follows:

1) Given the current state V' , find the time to the next transition for the envelope process as

$$\tau = -\ln(\mathfrak{R})/R^*$$

where \mathfrak{R} is a uniformly distributed random value in $(0, 1)$. The random variable τ is exponentially distributed with $\langle \tau \rangle = 1/R^*$.

2) Choose the new state, V , from the distribution $P^*(V|V')$.

3) With probability $W(V|V')/W^*(V|V')$ the transition $V' \rightarrow V$ occurs, otherwise, the event is a null event and the state V' is unchanged. In either case, the time is advanced by τ .

4) Return to step 1) until the required number of iterations are performed.

Note that the probability of a transition $V' \rightarrow V$ being selected in step 2) is $P^*(V|V')$ and the probability of that transition being accepted in step 3) is W/W^* so the net probability of the accepted transition is

$$P^*(V|V') \frac{W(V|V')}{W^*(V|V')} = P^*(V|V') \frac{W(V|V')}{R^* P^*(V|V')} = \frac{1}{R^*} W(V|V')$$

Since the total rate (accepted plus null transitions) is R^* the algorithm produces the stochastic process with the desired transition rate $W(V|V')$.

Clearly, the method will be inefficient if the ratio W/W^* is small since most transitions would be rejected. On the other hand, the method is only correct if $W/W^* \leq 1$ for all V, V' since the probability of acceptance cannot be greater than one (i.e., the null process cannot have negative probability for any V'). As such, the form of the envelope process (e.g., the mean and variance of the Gaussian) must be chosen with care.

-
- [1] J.C. Maxwell, *Theory of Heat*, (Longmans, Green and Co., London, 1871), chapter 12.
 - [2] L. Onsager, Phys. Rev. **37**, 405 (1931), Phys. Rev. **38**, 2265 (1931).
 - [3] P. A. Skordos, Phys. Rev. **E 48**, 777 (1993); K. Zhang and K. Zhang, Phys. Rev. **A 46**, 4598 (1993).
 - [4] L. Szilard, Z. Physik **53**, 840, (1929).
 - [5] R. Landauer, IBM J. Res. Dev. **5**, 183 (1961); C.H. Bennett, Int. J. Theor. Phys. **21**, 905 (1982); M. O. Magasco, Europhys. Lett. **33** 583 (1996).
 - [6] T.M. Nieuwenhuizen and A.E. Allahverdyan, Phys. Rev. **E 66**, 36102 (2002).
 - [7] P. Reimann, Phys. Rep. **361**, 57 (2002).
 - [8] M. v. Smoluchowski, Physik. Zeitschr. **13**, 1069 (1912); R. P. Feynman, R. B. Leighton, and M. Sands, *The Feynman Lectures on Physics I*, (Addison-Wesley, Reading, MA, 1963), chapter 46; C. Jarzynski and O. Mazonka, Phys. Rev. **E 59**, 6448 (1999).
 - [9] C.T.J. Alkemade, N.G. van Kampen and D.K.C. Mac Donald, Proc. Roy. Soc. **A 271**, 449 (1963).
 - [10] N. G. van Kampen, *Stochastic Processes in Physics and Chemistry*, (North-Holland, Amsterdam, 1981).
 - [11] I.M. Sokolov, Europhys. Lett. **44**, 278 (1999), Phys. Rev. **E 60**, 4946 (1999).
 - [12] J. Piasecki and C. Gruber, Physica **A 265**, 463 (1999); E. Kestemont, C. Van den Broeck, and M. Malek Mansour, Europhys. Lett. **49**, 143 (2000); T. Munakata and H. Ogawa, Phys. Rev. **E 64**, 036119 (2001); J.A. White, F.L. Roman, A. Gonzalez and S. Velasco, Europhys. Lett. **59**, 479 (2002); A.V. Plyukhin and J. Schofield, Phys. Rev. **E 69**, 021112 (2004).
 - [13] H. Callen, *Thermodynamics and an Introduction to Thermostatistics*, Second Edition (Wiley, New York, 1985).
 - [14] Ch. Gruber and J. Piasecki, Physica **A 268**, 412 (1999).
 - [15] K. Handrich and F.P. Ludwig, J. Stat. Phys. **86**, (1997).
 - [16] C. Van den Broeck, R. Kawai and P. Meurs, *Microscopic analysis of a thermal Brownian motor*, to appear in Phys. Rev. Lett.
 - [17] J. R. Dorfman, H. Van Beijeren, and C. F. McClure, Archives of Mechanics **28**, 333 (1976).
 - [18] J. M. R. Parrondo and P. Espagnol, Am. J. Phys. **64**, 1125 (1996); C. Van den Broeck, E. Kestemont, and M. Malek Mansour, Europhys. Lett. **56**, 771 (2001).
 - [19] S.N. Ethier and T.G. Kurtz, *Markov Processes, Characterization and Convergence* (Wiley, New York, 1986) pg. 163.